Thermal conductance of metal-metal interfaces

Bryan C. Gundrum, David G. Cahill,* and Robert S. Averback
Department of Materials Science and Engineering, and Frederick Seitz Materials Research Laboratory, University of Illinois, Urbana, Illinois 61801, USA

(Received 8 August 2005; revised manuscript received 22 September 2005; published 30 December 2005)

The thermal conductance of interfaces between Al and Cu is measured in the temperature range $78 < T < 298$ K using time-domain thermoreflectance. The samples are prepared by magnetron sputter deposition of a 100 nm thick film of Al on top of layers of Cu on sapphire substrates. The chemical abruptness of the Al-Cu interface is systematically varied by ion-beam mixing using 1 MeV Kr ions. The thermal conductance of the as-deposited Al-Cu interface is 4 GW m^{-2} K^{-1} at room temperature, an order-of-magnitude larger than the phonon-mediated thermal conductance of typical metal-dielectric interfaces. The magnitude and the linear temperature dependence of the conductance are described well by a diffuse-mismatch model for electron transport at interfaces.

DOI: 10.1103/PhysRevB.72.245426 PACS number(s): 73.40.Jn, 72.15.Eb, 78.20.Nv

I. INTRODUCTION

The transport of heat across interfaces between materials has typically been studied within the framework of heat transport by lattice vibrations.[1,2] Except for the case of materials with highly dissimilar vibrational spectra,[3] theoretical descriptions of specular and diffuse phonon scattering provide a reasonably good description of heat transport at interfaces between two dielectrics or interfaces between a metal and a dielectric.[4] At an interface between two *metals*, however, we can expect that electrons will contribute significantly to heat transport.[5] Charge and spin transport at interfaces has received significant attention by experiment[6–9] and theory[10–13]—particularly, in the context of so-called current-perpendicular-to-plane magnetoresisitive sensors—but heat transport between metals has received much less attention and prior experimental results have not been quantitative.[14] Here we provide data and employ a simple theoretical model, an electronic version of the "diffuse-mismatch model,"[1] which successfully describes the magnitude and temperature dependence of the heat transport. We estimate that phonons contribute $<10\%$ to the transport of energy across interfaces between typical metals. Therefore, in most cases, charge transport and heat transport at interfaces can be related by an extension of the Wiedemann-Franz law.[5]

We characterize heat transport at interfaces by the thermal conductance per unit area of the interface G; G is a linear transport coefficient that relates the heat flux J crossing the interface to the temperature drop ΔT at the interface, $J = G\Delta T$. We measure this fundamental transport property of the interface using time-domain thermoreflectance (TDTR), a pump-probe optical technique that measures the time evolution of the surface temperature through temperature-dependent changes in the optical reflectivity of the surface. TDTR has been applied in measurements of thermal transport for nearly 20 years;[15,16] we have recently advanced the state of the art of TDTR through improvements in methods used for data acquisition and analysis.[4,17]

We prepare samples for our studies by magnetron sputter deposition of metal layers on sapphire substrates. The relatively high thermal conductivity of sapphire dissipates the steady-state heating by the laser, which is on the order of 2 mW in a 13 μm diam focal spot. The sapphire substrate is first covered with a 3 nm thick Ti layer to improve adhesion between the sapphire and metal layers. Next, a layer of Cu (either $\approx$200 nm or $\approx$1.5 μm thick) is deposited, followed by an $\approx$100 nm thick layer of Al. Cu is chosen for the first metal layer because of its high thermal conductivity and the fact that Cu surfaces are relatively insensitive to contamination by residual gases in the high-vacuum sputtering chamber. Thus, we do not require UHV conditions to prepare a clean metal-metal interface. Al is chosen for the top layer because Al has high thermal conductivity and the thermoreflectance of Al, dR/dT, is large at the near-infrared wavelengths of the Ti:sapphire laser used for the measurements.

We systematically vary the chemical abruptness of the Al-Cu interface of the thick Cu sample by ion-beam mixing using 1 MeV Kr ions. The ion dose required to create a 10 nm thick interface layer by ion-beam mixing[18] is $\sim 5 \times 10^{15}$ cm^{-2}. We do not expect ion bombardment to change the thermal conductivity of the Cu or Al layers significantly.[19] The range of 1 MeV Kr ions in Cu is $\approx$300 nm and, therefore, ion bombardment under these conditions does not affect the Cu-sapphire interface.

II. MEASUREMENT TECHNIQUE AND DATA ANALYSIS

Our measurement technique and method for data analysis have been described previously[4,20] and applied in measurements of the thermal conductance of interfaces,[4] the thermal conductivity of thin films,[17,21–23] and high-resolution mapping of the thermal conductivity of combinatorial samples.[24] Briefly, the output of a mode-locked Ti:sapphire laser operating at a wavelength of 770 nm is split into two paths. The pump beam passes through an electro-optic modulator, a variable optical delay, and is focused onto the sample by a $10\times$ long working-distance microscope objective. The same objective lens that focuses the pump beam also focuses the probe beam, collimates the reflected probe beam, and forms a dark-field optical image of the sample surface on a CCD camera. The $1/e^2$ radius of the focused spots is 6.5 μm. The

small changes in the intensity of the reflected probe beam created by the pump beam are measured using lock-in detection at the 10 MHz modulation frequency of the pump beam. To eliminate background signals created by scattered light, we also modulate the probe beam at ≈200 Hz with a mechanical chopper; the in-phase and out-of-phase signals from the rf lock-in amplifier are then measured by two audiofrequency lock-in amplifiers locked to the frequency of the mechanical chopper.

We analyze the ratio of the in-phase V_{in} and out-of-phase V_{out} signals using an analytical solution of heat flow in a layered structure in cylindrical coordinates; the analytical solution can accommodate any number of layers.[20] The thermal response is first evaluated in the frequency domain and then transformed to the time-domain for comparisons between the model and the data; the lowest frequency component of the thermal response that contributes to the signal is the 10 MHz modulation frequency of the pump beam.[20] Because the diameter of the laser spot is large when compared to the thermal diffusion distance during the modulation period of the pump beam, heat flow is primarily one-dimensional in the through-thickness direction. Our approach of analyzing V_{in}/V_{out} instead of V_{in} alone greatly improves the sensitivity of our measurements to the thermal properties of the sample and also minimizes artifacts at long delay times created by changes in the spot size of the pump beam.

The thermal model includes parameters for the thermal conductivity, heat capacity, and thicknesses of the Al and Cu layers. The heat capacities are weakly dependent on microstructure, and we use the properties of bulk materials.[25,26] We add an additional 3 nm of Al to approximate the heat capacity contributed by the native oxide of Al. The thermal conductivities of the Al and Cu layers are estimated from the measured electrical resistivity at room temperature, the electrical resistance of the pure elements, and the Wiedemann-Franz law, which relates the electrical conductivity σ and thermal conductivity, $\Lambda = L\sigma T$, where $L = (\pi^2/3)(k_B^2/e^2)$ is the Lorenz number. For pure single crystals of Cu, the Wiedemann-Franz law provides an accurate description of the thermal conductivity at room temperature, but, at 80 K, the thermal conductivity of pure Cu is ≈30% smaller than predicted by the Wiedemann-Franz law.[26] The electrical resistivity of our metal films, however, is significantly increased by elastic scattering by impurities and other defects; the resistivity at 80 K is a factor of ≈2 larger than the intrinsic resistivity. Since we expect elastic scattering by defects to improve the reliability of the Wiedemann-Franz prediction, the Wiedemann-Franz law should be accurate to ≈15% over the entire temperature range of our measurements. The thermal conductivity and heat capacity of the sapphire substrate are taken from Refs. 27 and 28, respectively. Thicknesses of the Al and Cu layers are measured by picosecond acoustics and Rutherford backscattering spectroscopy.

This procedure leaves two unknowns in the thermal analysis: the thermal conductance of the Al-Cu interface and the thermal conductance of the Cu-sapphire interface. (We refer to the bottom interface as the Cu-sapphire interface but remind the reader that this interface includes a 3 nm thick layer of Ti in between the Cu layer and the sapphire substrate to improve adhesion.) Measurements of heat transport in samples with thin Cu layers are sensitive to the thermal conductance of both interfaces. To measure the thermal conductance of the Al-Cu interface, we use a much thicker Cu layer, 1.5 μm thick, to reduce the influence of the conductance of the Cu-sapphire interface on the data. The conductance of the Cu-sapphire interface and the thermal properties of the sapphire substrate are relatively unimportant when the thermal penetration depth l in the Cu layer is smaller than the Cu layer thickness; $l = \sqrt{D/\omega} \approx 1$ μm, where $D \approx 1$ cm^2 s^{-1} is the thermal diffusivity of the Cu layer and $\omega = 2\pi \times 10^7$ s^{-1} is the angular frequency of the modulation of the pump-beam.

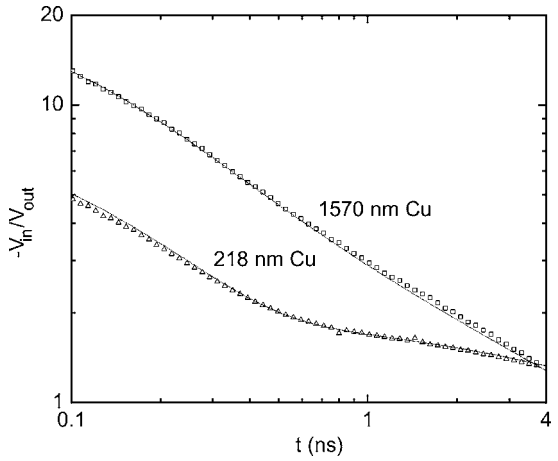

FIG. 1. Ratio of the in-phase and out-of-phase changes in the intensity of the probe beam plotted as a function of the time delay between the pump and probe optical pulses. Each curve is labeled by the thickness of the Cu layer. The dashed lines are fits to the thermal model used to determine the thermal conductance of the Al-Cu and Cu-Al_2O_3 interfaces.

Figure 1 shows the fits of the thermal model to the data for the two samples with different thicknesses of the Cu layer, and Fig. 2 shows the sensitivity of these fits to changes in the various parameters in the thermal model. We define the sensitivity of the fit S_α as the logarithmic derivative of V_{in}/V_{out} with respect to one of the parameters. If that parameter is labeled α, then

$$S_\alpha = \frac{d \ln(-V_{in}/V_{out})}{d \ln \alpha}. \quad (1)$$

For the thicker layer of Cu, the maximum of the sensitivity of V_{in}/V_{out} to changes in G of the Al-Cu interface at room temperature is ≈−0.2 at delay times near 300 ps; in other words, a 5% increase in G produces a 1% decrease in V_{in}/V_{out} near $t = 300$ ps. The sensitivity is larger at lower temperatures, ≈−0.5 at 78 K (data not shown).

III. RESULTS AND THE DIFFUSE MISMATCH MODEL FOR ELECTRONS

The experimental results for G are plotted as a function of the measurement temperature in Fig. 3. The conductance of the Al-Cu interface at room temperature is 4 GW m^{-2} K^{-1}, a factor of ≈7 larger than the largest thermal conductance

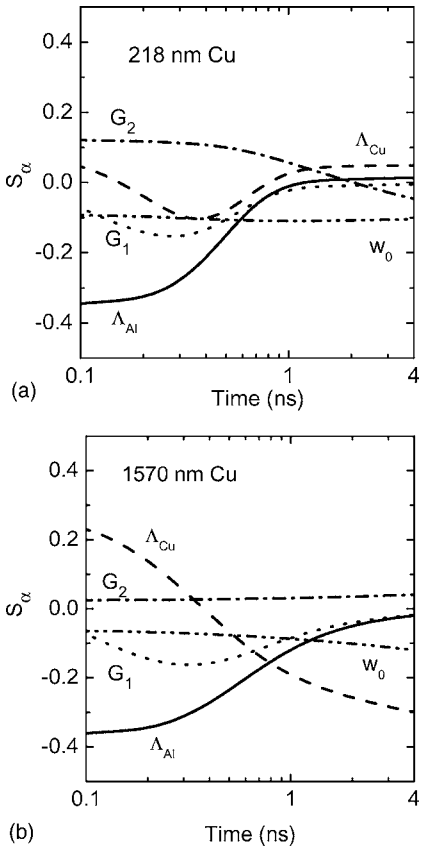

FIG. 2. The sensitivity of V_{in}/V_{out} to changes in selected parameters in the thermal model as calculated by Eq. (1). (a) Sensitivities at room temperature for the "thin Cu" sample, and (b) sensitivities at room temperature for the "thick Cu" sample. G_1 and G_2 are the Al-Cu and Cu-Al_2O_3 interface conductances; w_0 is the spot size, and Λ_{Al} and Λ_{Cu} are the thermal conductivities of the Al and Cu layers.

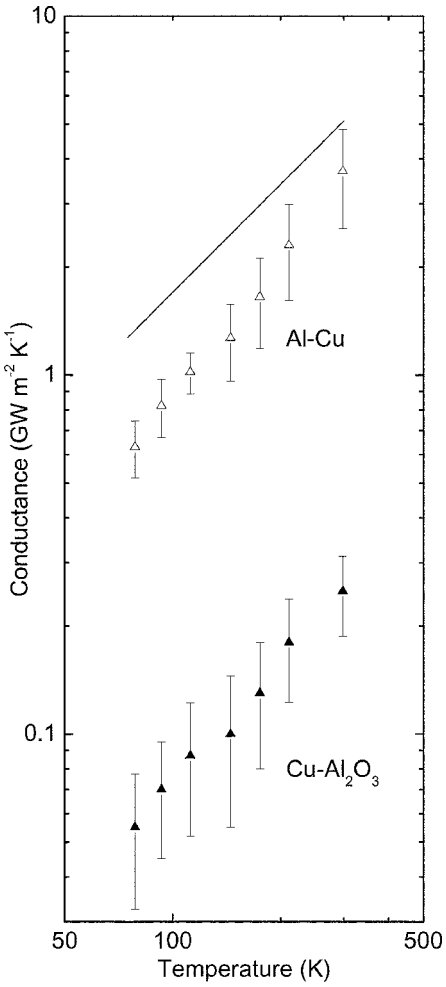

FIG. 3. Thermal conductance of the Al-Cu (open symbols) and Cu-Al_2O_3 (filled symbols) interfaces as a function of the measurement temperature. The data are obtained by the combination of measurements on the two samples with different Cu layer thickness. The solid line shows the predictions for the conductance of the Al-Cu interface using the diffuse-mismatch model for electron transport described by Eq. (4).

measured to date for energy transport by lattice vibrations across TiN-MgO interfaces[4] and a factor of ≈20 times larger than the conductance of more typical combinations of metals and dielectrics: in our experience with a large number of combinations of metals and dielectrics, the phonon-mediated thermal conductance typically falls in the range $0.08 < G < 0.30$ GW m^{-2} K^{-1}. (Interfaces with Pb or Bi are an exception; in this case G is an order of magnitude smaller,[29] $0.008 < G < 0.030$ GW m^{-2} K^{-1}.)

To understand the magnitude of the thermal conductance, we follow previous work[1] on phonon-mediated thermal conductance and make the simplifying assumption that all electrons are scattered diffusely and elastically at the interface; in other words, we do not consider conservation of crystal momentum, but we do require that the incident and scattered electrons have the same energy. We do not know if this is an accurate description of the transport of Al-Cu interfaces, but recent theoretical studies[11,13] have reached the conclusion that a majority of electrons are scattered diffusely when the width of the random alloy that forms at the interface is a few atomic-layers thick. We expect that the as-deposited Al-Cu interfaces are both geometrically rough and chemically diffuse.

The assumption of diffuse scattering of phonons is the basis of the so-called diffusive-mismatch model[1] (DMM) commonly used to described the phonon-mediated transport of heat at interfaces. An extension of the DMM model to electron transport is straightforward. Detailed balance requires that the averaged transmission coefficient of an electron with energy E is given by terms involving the products of the electron velocities v_i and the densities of states $D_i(E)$ on both sides of the interface. This approach does not require ballistic transport over the entire thickness of the sample, only locally at the interface. For example, the transmission coefficient Γ_1 from material 1 to material 2 is

$$\Gamma_1(E) = \int_0^{\pi/2} \frac{v_2(E)D_2(E)}{v_1(E)D_1(E) + v_2(E)D_2(E)} \cos\theta \sin\theta d\theta. \quad (2)$$

If we make the further simplification of a degenerate metal

with an isotropic Fermi surface, the thermal conductance of the interface is

$$G = \frac{1}{2} v_1(E_F)\Gamma_1(E_F)\int_0^\infty E\frac{dN_1(E,T)}{dT}dE, \tag{3}$$

where $N_1(E,T)$ is the density of occupied states of energy E at temperature T. The integral is the same as the electronic heat capacity per unit volume C_e and, since for a degenerate electron gas, C_e is proportional to $D(E_F)$ and temperature T, $C_e=(\pi^2/3)D(E_F)k_B^2T=\gamma T$, we write G in the form

$$G = \frac{Z_1 Z_2}{4(Z_1+Z_2)}, \tag{4}$$

where Z_i is given by the product of the electronic heat capacity per unit volume γT and Fermi velocity v_F of side i; $Z=\gamma v_F T$. We assume that the density of states is independent of temperature. We use low-temperature measurements of γ, calculated values of the average value of v_F for Al[30] and assume that v_F for Cu is given by the free electron value. Then, $Z_{Al}=0.18T$, $Z_{Cu}=0.11T$, and $G=0.017T$, where Z and G are in units of GW m^{-2} K^{-1} when T is expressed in degrees Kelvin. This simple model produces a remarkably good description of the thermal conductance of the as-deposited Al-Cu interface, see Fig. 3. The temperature dependence of the data is slightly steeper than a linear dependence on temperature, but the discrepancy at 78 K is small, only $\approx$15%.

Since large γ tends to be associated with high effective mass and small v_F, the product γv_F will show less variations between metals than either γ or v_F alone.

The interface form of the Wiedemann-Franz law is[5]

$$\frac{G(AR)}{T} = L, \tag{5}$$

where AR is the specific electrical resistance of the interface,[7–9] and L is the Lorentz number, 2.45×10^{-8} Ω W K^{-2}. A linear temperature dependence for G is then consistent with a temperature-independent specific electrical resistance (AR) and using Eq. (5), we derive $AR=1.8$ $f\Omega$ m^2 for the as-deposited Al-Cu interfaces. This value of AR for Al/Cu is comparable to AR measured for Cu/W interfaces by electrical transport through Cu/W multilayers;[8] larger by a factor of $\approx$5 than AR measured for Pd/Ag and Pd/Au multilayers;[9] and larger by a factor of $\approx$40 than AR measured for Ag/Cu and Ag/Au multilayers.[7]

IV. ION-IRRADIATED INTERFACES

By introducing ion bombardment, we can expect that the interface conductance will eventually approach the conductance Λ_{AlCu}/δ of the intermixed interfacial layer, where Λ_{AlCu} is the thermal conductivity of the intermixed interface layer and δ is its thickness. Furthermore, we expect δ to scale with the square root of the ion dose F. To test this idea, we fit the data plotted in Fig. 4 using a function of the form

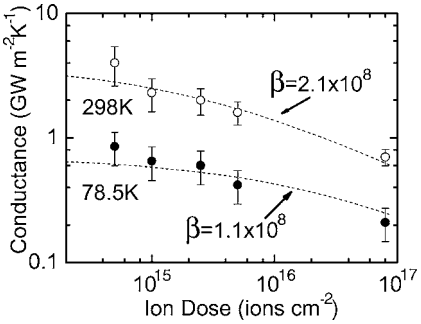

FIG. 4. Thermal conductance of Al-Cu interfaces as a function of ion dose. Each curved is labeled by the measurement temperature in degrees Kelvin. The dashed lines are fits to the data to determine the value of the parameter β in Eq. (6); β is given in units of GW m^{-2} cm^{-1} K^{-1}.

$$\frac{1}{G} = \frac{1}{G_0} + \frac{F^{1/2}}{\beta}, \tag{6}$$

where G_0 is the conductance of the as-deposited sample. We find $\beta=2.4\times10^8$ GW m^{-2} cm^{-1} K^{-1} at room temperature and $\beta=1.1\times10^8$ GW m^{-2} cm^{-1} K^{-1} at 78 K.

Previous studies by Chang *et al.* suggest that an Al-Cu interface will be dominated by a Al_4Cu_9 compound.[31] The resistivity of Al_4Cu_9 is $\approx$20 $\mu\Omega$ cm at room temperature[32] and the Wiedemann-Franz law then predicts $\Lambda_{AlCu}\approx36$ W m^{-1} K^{-1}. An ion dose of 3×10^{15} reduces the interface conductance from the as-deposited value by a factor of two; therefore, from the measurements of conductance we deduce $\delta=9$ nm at this ion dose, in good agreement with previous results.[31]

V. CONCLUSIONS

We find that the thermal conductance of a metal-metal interface is an order of magnitude larger than typical metal-dielectric interfaces and both the magnitude and the temperature dependence of the conductance are in good agreement with a diffuse-mismatch model for electron transport at interfaces. Since transport at metal interfaces will often be controlled by elastic scattering by disorder—and the phonon contribution to the transport will be relatively small—the interface form of the Wiedemann-Franz law[5] may enable direct correlations between measurements of thermal and electrical transport through interfaces.

ACKNOWLEDGMENTS

This work was supported by the U.S. Department of Energy, Division of Materials Sciences under Grant No. DEFG02-91ER45439, through the Frederick Seitz Materials Research Laboratory (MRL) at the University of Illinois at Urbana-Champaign. Sample characterization used the facilities of the Center for Microanalysis of Materials, which is partially supported by the U.S. Department of Energy under Grant No. DEFG02-91ER45439; and the Laser Facility of the MRL.

*Electronic address: d-cahill@uiuc.edu

[1] E. T. Swartz and R. O. Pohl, Rev. Mod. Phys. **61**, 605 (1989).
[2] D. G. Cahill, W. K. Ford, K. E. Goodson, G. D. Mahan, A. Majumdar, H. J. Maris, R. Merlin, and S. R. Phillpot, J. Appl. Phys. **93**, 793 (2003).
[3] R. J. Stoner and H. J. Maris, Phys. Rev. B **48**, 16373 (1993).
[4] R. M. Costescu, M. A. Wall, and D. G. Cahill, Phys. Rev. B **67**, 054302 (2003).
[5] G. D. Mahan and M. Bartkowiak, Appl. Phys. Lett. **74**, 953 (1999).
[6] W. P. Pratt Jr., Q. Yang, L. L. Henry, P. Holody, W.-C. Chiang, P. A. Schroeder, and J. Bass, J. Appl. Phys. **79**, 5811 (1996).
[7] L. L. Henry, Q. Yang, W.-C. Chiang, P. Holody, R. Loloee, W. P. Pratt Jr., and J. Bass, Phys. Rev. B **54**, 12336 (1996).
[8] W. Park, D. V. Baxter, S. Steenwyk, I. Moraru, W. P. Pratt, Jr., and J. Bass, Phys. Rev. B **62**, 1178 (2000).
[9] C. Galinon, K. Tewolde, R. Loloee, W. C. Chiang, S. Olson, H. Kurt, W. P. Pratt, Jr., J. Bass, P. X. Xu, K. Xia, and M. Talanana, Appl. Phys. Lett. **86**, 182502 (2005).
[10] A. Shpiro and P. M. Levy, Phys. Rev. B **63**, 014419 (2000).
[11] V. Drchal, J. Kudrnovsky, P. Bruno, P. H. Dederichs, I. Turek, and P. Weinberger, Phys. Rev. B **65**, 214414 (2002).
[12] G. E. W. Bauer, K. M. Schep, K. Xia, and P. J. Kelly, J. Phys. D **35**, 2410 (2002).
[13] J. Velev and W. H. Butler, Phys. Rev. B **69**, 024404 (2004).
[14] B. M. Clemens, G. L. Eesley, and C. A. Paddock, Phys. Rev. B **37**, 1085 (1988).
[15] C. A. Paddock and G. L. Eesley, J. Appl. Phys. **60**, 285 (1986).
[16] D. A. Young, C. Thomsen, H. T. Grahn, H. J. Maris, and J. Tauc, in *Phonon Scattering in Condensed Matter*, edited by A. C. Anderson and J. P. Wolfe (Springer, Berlin, 1986), p. 49.
[17] D. G. Cahill and F. Watanabe, Phys. Rev. B **70**, 235322 (2004).
[18] B. M. Paine and R. S. Averback, Nucl. Instrum. Methods Phys. Res. B **7-8**, 666 (1985).
[19] R. C. Birtcher and T. H. Blewitt, J. Nucl. Mater. **98**, 63 (1981).
[20] D. G. Cahill, Rev. Sci. Instrum. **75**, 5119 (2004).
[21] R. M. Costescu, D. G. Cahill, F. H. Fabreguette, Z. A. Sechrist, and S. M. George, Science **303**, 989 (2004).
[22] D. G. Cahill, F. Watanabe, A. Rockett, and C. B. Vining, Phys. Rev. B **71**, 235202 (2005).
[23] X. Zheng, D. G. Cahill, and J.-C. Zhao, Adv. Eng. Mater. **7**, 622 (2005).
[24] S. Huxtable, D. G. Cahill, V. Fauconnier, J. O. White, and J.-C. Zhao, Nat. Mater. **3**, 298 (2004).
[25] W. F. Giauque and P. F. Meads, J. Am. Chem. Soc. **63**, 1897 (1941).
[26] J. P. Moore, D. L. McElroy, and R. S. Graves, Can. J. Phys. **45**, 3849 (1967).
[27] D. G. Cahill, S.-M. Lee, and T. I. Selinder, J. Appl. Phys. **83**, 5783 (1998).
[28] G. S. Parks and K. K. Kelley, J. Phys. Chem. **30**, 47 (1926).
[29] H.-K. Lyeo and D. G. Cahill (unpublished).
[30] B. Sundqvist, J. Neve and Ö. Rapp, Phys. Rev. B **32**, 2200 (1985).
[31] C. T. Chang, S. U. Campisano, S. Cannavó, and E. Rimini, J. Appl. Phys. **55**, 3322 (1984).
[32] C. Macchioni, J. A. Rayne, and C. L. Bauer, Phys. Rev. B **25**, 3865 (1982).